Pt redistribution in Ni(Pt)Si layers obtained via total vs partial reactions and its impact on specific contact resistivity

Sophie Guillemin [a]*, Lillà Ferreint-Roselli [a], Patrice Gergaud [a], Nicolas Bernier [a], Isabelle Tinti [a], Cédric Bomme [a], Nicolas Gauthier [a], Philippe Rodriguez [a]

[a] *Univ. Grenoble Alpes, CEA-LETI, 38000 Grenoble, France*

Ni(Pt)Si layers are often used as contact layers in CMOS technologies. Historically, they were obtained using a single annealing. Currently, the associated process is rather based on two annealings, allowing to perform partial reactions, meaning that not all the deposited metal is of actual use [1]. After metal deposition, the first annealing is performed, during which part of the deposited Ni layer reacts with the substrate. It is followed by a selective etch, which removes the remaining metal. The second annealing allows to obtain the desired low-resistive Ni(Pt)Si phase. The impact of this change in terms of grown Ni(Pt)Si layer properties and associated contact performances is not well known. Yet, the redistribution of Pt in the system should be impacted, since Pt is expected to segregate at the $Ni_{1-x}(Pt)Si_x$ surface, a mechanism known as the snowplow effect [2].

In order to gain understanding on this topic, $Ni_{0.9}Pt_{0.1}$ metal layers of various thicknesses were deposited on top of 300 mm n-doped Si(100) wafers. A two-step annealing process based on rapid thermal annealings (RTA) was defined: RTA1 at 230 °C for 20 s and RTA2 at 390 °C for 30 s. The first annealing should consume around 5 nm of $Ni_{0.9}Pt_{0.1}$. The thickness of the deposited metal layer was varied from 5 nm to 22 nm (see Fig. 1), allowing not only to compare a total vs a partial reaction, but also to understand the role of the available metal reservoir. The layers were characterized after RTA1 and RTA2 via XRD measurements. After RTA2, additional XRR, SEM and TOF-SIMS measurements were performed. The same set of conditions was then applied on patterned wafers defining TLM structures [3]. The specific contact resistivity (ρ_c) of the n-doped $Si/Ni_{1-x}(Pt)Si_x$ interface was obtained and complementary TEM analyses were performed on two relevant samples.

On blanket wafers, it is shown that the thickness of the Ni(Pt)Si layers obtained using the procedure described here above is equivalent for all the samples, despite slightly lower for S1 and, in a lesser extent, S2 (see Fig. 1). The layers present a similar texture, with two preferential orientations out of the plane along the [010] and [013] crystalline directions, and some degree of epitaxy (not shown). Such a texture is indicative of a growing mechanism involving the sequential development of nanocrystalline phases (see also XRD data collected post RTA1, presented Fig. 2). However, the average diameter of the grains composing the Ni(Pt)Si layers and obtained via SEM image analysis (not shown) varies along the samples. The biggest grains are obtained for sample S1, with a mean value of 77 nm ± 33 nm, for then quickly drop (mean value of 45 nm ± 18 nm for S2 and 42 nm ± 13 nm for S5). More importantly, the redistribution of Pt is not equivalent for all samples. As expected, Pt strongly segregates at the Ni(Pt)Si surface (see Fig. 3(a)ii)). But, overall, less Pt is incorporated in S1 and, in a lesser extent, S2. Additionally, S1 is the only sample showing a slight Pt signal at the bottom Ni(Pt)Si/Si interface (see Fig. 3(b)). On patterned wafers, it is shown Fig. 4(a) that ρ_c is not equivalent for all the samples, with best results obtained for partial reactions. While some trends are not preserved as compared to blanket wafers (sample average grain size, see diffraction patterns presented Fig. 4(b)), Pt atom redistribution is clearly impacted (see Fig. 4(b), EDX maps). The presence of Pt atoms at the bottom Ni(Pt)Si/Si interface is proposed to drive ρ_c observed differences.

Acknowledgements: Part of this work, carried out on the Platform for Nanocharacterisation (PFNC), was supported by the ‘‘Recherche Technologique de Base’’ and ‘‘France 2030 - ANR-22-PEEL-0014’’ programs of the French National Research Agency (ANR).

References

1. F. Morris Anak, A. Campos, M. Grégoire, A. Estellon, M. Lombard, T. Guyot, S. Guillemin and D. Mangelinck, *MAT SCI SEMICON PROC* **184**, 108806 (2024)
2. O. Cojocaru-Mirédin, D. Mangelinck, K. Hoummada, E. Cadel, D. Blavette, B. Deconihout and C. Perrin-Pellegrino, *SCRIPTA MATER* **57 (5)**, 373-376 (2007).
3. S. Guillemin, L. Lachal, P. Gergaud, A. Grenier, F. Nemouchi, F. Mazen and P. Rodriguez, *MICROELECTRON ENG* **291**, 112210 (2024)

* *corresponding author e-mail: sophie.guillemin@cea.fr*

	Sample name				
	S1	S2	S3	S4	S5
Deposited metal thickness (nm)	5	7	10	14	22
XRR results					
Ni(Pt)Si layer thickness (nm)	11.4	11.8	11.9	11.9	11.9
Ni(Pt)Si layer roughness (nm)	3.8	3.5	2.8	2.5	2.4
Ni(Pt)Si layer density (g/cm³)	20.1	20.7	20.8	20.6	21.0
Top layer	7.1	7.5	7.7	7.8	7.9
Middle layer	6.5	6.7	6.7	6.6	6.7
Bottom layer	6.5	6.4	6.3	6.2	6.4

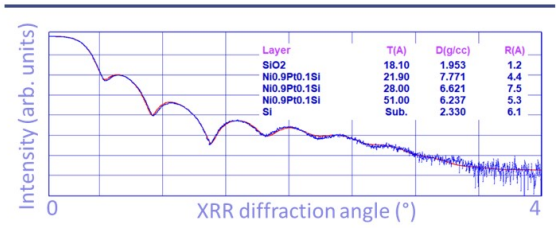

Fig. 1: Presentation of the studied samples and corresponding XRR results post RTA2 (top). Example of data fitting for S3 (bottom). The fits are performed using a 3 layers model, which should reflect the expected Pt gradient within the Ni(Pt)Si layer. The given layer thickness values are the sum of the 3 contributions. Due to air break between RTA2 and XRR measurement, a SiO_2 layer is added on top of the structure, in order to account for oxidation phenomena. The given layer roughness values are the sum of all contributions.

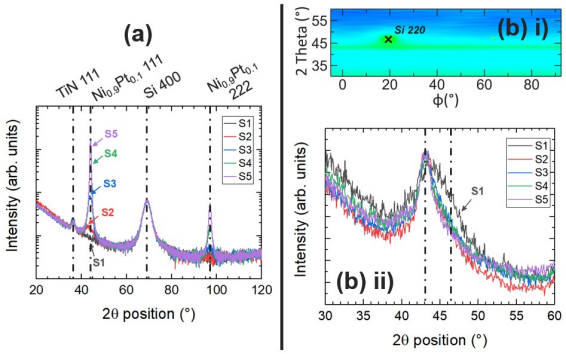

Fig. 2: XRD results obtained post RTA1, before selective etch. (a) Out-of-plane acquisition in ω-2θ configuration. (b) i) In-plane reciprocal space map (IPRSM) of sample S4, given here as an example. All the samples show the same signature, i.e. a weak signal arranged along a fiber texture around 43°. ii) IPRSM diffraction signal integrated over the whole investigated φ range for the whole sample set, with the Si epitaxial spots cut out in the process in order to avoid their parasitic contribution. No strong signal that would be associated to a grown Ni-rich phase is seen, neither in-plane nor out-of-plane, which means that the layer presents a nano-crystalline structure.

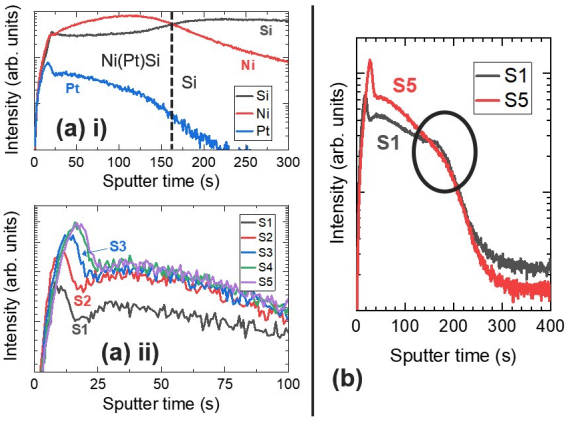

Fig. 3: (a) TOF-SIMS analysis using a primary Bi_3^+ ion source and Cs^+ sputtering source showing i) a general overview of the system (example of S4) and ii) a comparative study of Pt segregation amount at the top interface. The bottom Ni(Pt)Si/Si interface is not resolved with this acquisition conditions. (b) Comparative Pt TOF-SIMS analysis using a primary Cs- ion source of S1 and S5. The bottom interface is resolved and shows the presence of Pt atoms for S1 only.

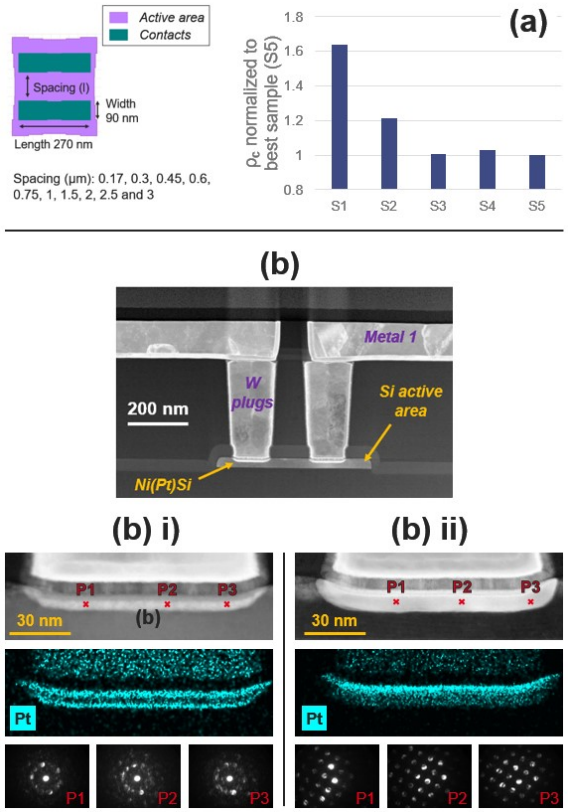

Fig. 4: (a) Top-view of the TLM design used for electrical characterization (left). Degradation of the specific contact resistivity when available metal for siliciuration is reduced, with ρ_c = 4.9E-8 Ω.cm² for S5 (right). (b) BF-STEM image of a representative TLM motif and zoom on the contact area with associated Pt EDX mapping and diffraction spots for contact process conditions equivalent to i) sample S1 (total reaction) and ii) sample S4 (partial reaction).